Analysis of MAP 4 Function in Living Cells Using Green Fluorescent Protein (GFP) Chimeras

Keith R. Olson,* J. Richard McIntosh,‡ and J. B. Olmsted*

*Department of Biology, University of Rochester, Rochester, New York 14627; and ‡Molecular, Cellular, and Developmental Biology, University of Colorado, Boulder, Colorado 80309

Abstract. MAP 4 is a ubiquitous microtubule-associated protein thought to play a role in the polymerization and stability of microtubules in interphase and mitotic cells. We have analyzed the behavior of protein domains of MAP 4 in vivo using chimeras constructed from these polypeptides and the green fluorescent protein (GFP). GFP-MAP 4 localizes to microtubules; this is confirmed by colocalization of GFP-MAP 4 with microtubules that have incorporated microinjected rhodamine-tubulin, and by loss of localized fluorescence after treatment of cells with anti-microtubule agents. Different subdomains of MAP 4 have distinct effects on microtubule organization and dynamics. The entire basic domain of MAP 4 reorganizes microtubules into bundles and stabilizes these arrays against depolymerization with nocodazole. Within the basic domain, the PGGG repeats, which are conserved with MAP 2 and tau, have a weak affinity for microtubules and are dispensable for microtubule binding, whereas the MAP 4-unique PSP region can function independently in binding. The projection domain shows no microtubule localization, but does modulate the association of various binding subdomains with microtubules. The acidic carboxy terminus of MAP 4 strongly affects the microtubule binding characteristics of the other domains, despite constituting less than 6% of the protein. These data show that MAP 4 association with microtubules is modulated by sequences both within and outside the basic domain. Further, our work demonstrates that GFP chimeras will allow an in vivo analysis of the effects of MAPs and their variants on microtubule dynamics in real time.

PROPER assembly and organization of the microtubule cytoskeleton are required for cellular processes such as mitosis, organelle transport, and the establishment of cell shape and polarity. For microtubules to function in such varied processes, they must be amenable to change and their lability must be controlled. The lability of microtubules derives from their dynamic instability, i.e., rapid changes between phases of depolymerization and regrowth (18, 26, 51). The control of dynamic instability and the selective stabilization of particular populations of microtubules are essential for the preservation of normal microtubule organization within cells (reviewed in reference 32). In some cases, stable and transient microtubules are characterized by post-translational modifications of tubulin (13, 23). Structural microtubule-associated proteins (MAP)[1] may also play essential roles in determining the in vivo characteristics of individual microtubules and dictating the state of microtubule assembly in a cell (20, 43, 54).

MAPs are identified by their copurification with tubulin and association with microtubules both in vitro and in vivo. They are divided into two broad categories: motor MAPs (the kinesin [5] and dynein [33] superfamilies) and structural MAPs (MAP1A, MAP1B, MAP 2, MAP 4, tau (reviewed in references 32, 43, 54), ensconsin (12), EMAP115 (49), X-MAP (2, 25). Structural MAPs are generically associated with increased microtubule assembly and stability, as demonstrated in a number of in vitro analyses. Studies in which the major neural MAPs, MAP 2 and tau, were either overexpressed in vivo in heterologous systems (37, 38, 40, 44, 62) or eliminated using antisense technology (16, 17) have further implicated these proteins in both microtubule stabilization and organization during neurogenesis. Recent results from knockout of the mouse tau gene indicate, however, that neural MAPs may be functionally redundant (31). MAP 4 is more ubiquitous than the neuronal MAPs, and its functions in cytoskeletal organization in vivo are unknown.

MAP 4 is a group of related thermostable polypeptides that migrate on polyacrylamide gels with an apparent M_r of 200–240 kD (8, 11, 53, 55). Its expression is nearly ubiquitous (10, 57) and it is localized to both interphase and

Address all correspondence to J. B. Olmsted, Dept. of Biology, University of Rochester, Rochester, NY 14627. Tel.: (716) 275-3440/4827. Fax: (716) 275-2070. e-mail: OLMJ@db1.cc.rochester.edu.

1. *Abbreviations used in this paper*: BD, basic domain of MAP 4; GFP, green fluorescent protein; HA, hemagglutinin; MAP, microtubule-associated protein; nt, nucleotide.

mitotic microtubules (9). MAP 4 polypeptides are encoded by a single gene from which multiple messages are transcribed (21, 63), and some of the protein isotype diversity arises from alternative splicing (reference 20 and unpublished data). Differences may also arise from cell cycle-dependent changes in MAP 4 phosphorylation (59, 60).

The presence and conservation of distinct protein domains within MAP 4 have been inferred from comparisons of sequences from human, mouse and bovine sources (63). MAP 4 has two major charge domains, an acidic domain that projects from the microtubule surface and a basic region that contains sequences responsible for microtubule binding (Fig. 1 *A*). The acidically charged NH_2-terminal projection domain consists principally of a region containing a variable number of 14–amino acid degenerate repeats (the KDM repeats); these are proposed to form multiple short α-helices. The extreme amino terminus of the protein (*N*) is a highly conserved domain of unknown function. The basic domain constitutes about one third of the protein. It comprises a region unique to MAP 4 and a region containing several 18-mer degenerate repeats (*PGGG*) that are similar to sequences found in MAP 2 and tau (46). Alternative splicing generates variations in the number and type of repeats, but this region has been considered the canonical microtubule binding domain in these MAPs (see in vitro binding studies in references 15, 22, 36). The portion of the basic domain unique to MAP 4 can be divided into two domains: a highly conserved region that is rich in proline (*P*) and a region abundant in serine and proline (*SP*). The latter region contains conserved sites of potential phosphorylation, including a consensus site for cdc2 kinase. MAP 4 also has a short acidic carboxy terminus (*C*) that is highly conserved across species, but it shares only minimal similarity with the corresponding terminal regions in other MAPs.

This paper describes the use of chimeras of MAP 4 and a recently discovered reporter molecule, green fluorescent protein (*GFP*), to examine the behavior of MAP 4 and its subdomains in living cells. GFP is a 238 amino acid protein from the jellyfish *Aequorea victoria*; it absorbs light at 395 and 470 nm, emits light prominently at 510 nm, and can be detected using standard epifluorescence filters for fluorescein (34, 58). The utility of GFP as a marker in living cells has been demonstrated in elegant studies on cellular migration in *Caenorhabditis elegans* (19) and particle movements during *Drosophila* oogenesis (61). Our in vivo analyses of GFP-MAP 4 chimeras demonstrate that this reporter molecule can also be used to track the subcellular reorganization of cytoskeletal elements. The lack of toxicity of these chimeras and the ability to select stable cell lines expressing GFP-MAP 4 has enabled us to determine the contributions made by individual MAP 4 domains to microtubule binding and organization in vivo.

Materials and Methods

Cell Culture

All cell lines were grown at 37°C with 5% CO_2 + 95% air in F-12 nutrient media supplemented with 10% fetal bovine serum. Cultures were split and passaged using standard trypsinization procedures.

Construction of Vectors for Expression of Tagged MAP 4 Domains

The constructs discussed in this paper are summarized in Fig. 1 *B*. GFP expression vectors were made in either pRc/CMV or pCR3 (Invitrogen, San Diego, CA) through PCR and subcloning. To generate vectors that would express GFP in mammalian cells, we initially made constructs that encoded GFP alone. The GFP coding region was amplified from the pGFP 10.1 plasmid (reference 19; generous gift of Dr. Martin Chalfie, Columbia University, NY) using a 5′ primer containing a HindIII restriction endonuclease site and the first 26 nt of GFP coding sequence, and a 3′ primer containing the last 20 nt of GFP coding sequence, excluding the stop codon, and either a NotI or HindIII restriction endonuclease site. In initial experiments, the amplimer was ligated directly to the epitope-tagged MAP 4 constructs described below using the HindIII sites. In subsequent experiments, the HindIII/NotI amplimers were used for ligation into pRc/CMV alone, or into MAP 4 constructs that had been generated by subcloning and/or PCR with NotI/ApaI sites. In these latter cases, the open reading frame between the 3′ end of the GFP coding region and the MAP 4 inserts was maintained by the addition of a single nucleotide at the 3′ side of the NotI site. The complete GFP sequence was confirmed by sequencing of the amplimer; it contained the substitution at position 264 reported previously (19). Constructs were restriction mapped and then sequenced at their ends to confirm the integrity of the GFP-MAP 4 chimeras.

Additional expression constructs were made through PCR amplification from existing GFP constructs using a 5′ GFP primer and MAP 4-specific 3′ primers, each with engineered translation termination codons and a 3′ ApaI restriction endonuclease site. For the PGGG and PGGGC constructs, MAP 4 sequences were PCR amplified with a 5′ NotI site and subcloned into pCR3 already containing GFP with the 3′ NotI restriction site. PCR products encoding GFP fused to all remaining MAP 4 sequences were subcloned according to manufacturer's protocol directly into the pCR3 vector included in the eukaryotic TA cloning kit (Invitrogen, San Diego, CA). All fusions were restriction mapped and sequenced at their ends to determine insert orientation and fidelity.

For some experiments, MAP 4 domains were generated with an epitope tag by making constructs incorporating the nine amino acid hemagglutinin (HA) sequence (YPYDVPDYA) from influenza virus (41); this is recognized by the 12CA5 mAb (Babco, Richmond, CA). The epitope was placed at the 5′ end of the basic domain (BD) of MAP 4, or 5′ to the PSP and PGGG regions of the MAP 4 BD separately, using PCR amplification with appropriate primers. Each 5′ primer contained a HindIII restriction endonuclease site, a translation initiator codon, the 27-nt sequence for the epitope, and sequence specific for the MAP 4 region of interest. The 3′ PCR primers for each construct encoded both a translation termination codon and an XbaI restriction endonuclease site. PCR products were purified, restriction digested, and used for subcloning into similarly digested pRc/CMV plasmid. After subcloning, all constructs were sequenced at both ends to ensure proper amplification of MAP 4 domains.

Transfection

All cell lines were transfected using Lipofectamine (GIBCO BRL, Gaithersburg, MD), with some minor modifications of the manufacturer's protocol. For Cos-7 cells, 1 μg of DNA was used with 8 μl of liposomes, while all other cells were transfected with 1 μg of DNA and 6 μl of liposomes. Purified DNA was prepared using columns (Qiagen, Chatsworth, CA), and for most transfections, serum-free DME was used in place of OPTI-MEM (GIBCO BRL) medium. Cells were incubated at 37°C and 5% CO_2 in the presence of DNA-liposome complexes for 2.5 h (5 h for Cos-7 cells), after which the solution was replaced with standard growth medium. Transfectants were then analyzed at various times for expression of exogenous protein. In some cases, cells were first allowed to recover for 5 h and were then treated with 2 mM sodium butyrate to enhance general transcription levels.

Selection of Stable Cell Lines

Both BHK and CHO cell lines were used for the isolation of cells stably expressing MAP 4 constructs. Cells with stably integrated plasmids were selected by growing transiently transfected cells in the presence of 2 mg/ml G418, a neomycin analogue (GIBCO BRL). Clonal isolates were obtained through serial dilution of stable transfectants into 96-well plates, after which they were amplified and seeded onto glass coverslips in 35-mm

dishes to monitor expression of GFP. Cells were maintained in medium containing 2 mg/ml G418.

Microinjection

Cells (PtK, 3T3, BHK, or Cos-7) grown on coverslips were microinjected as described previously (56) in a chamber that contained F-12 supplemented with 10% fetal bovine serum and 13 mM Hepes, pH 7.0. Construct DNA was injected at 1 mg/ml in PBS, pH 7.0, and in some experiments, 1 mg/ml Lucifer Yellow (Molecular Probes, Inc., Eugene, OR) was added to identify injected cells. Rhodaminated tubulin (28) with 3.9 mol rhodamine/tubulin dimer (obtained from Molecular Probes) was microinjected at a concentration of 1 mg/ml. These injections were performed in the absence of tracer dye on cells that were transiently transfected with the GFP-MAP 4 construct.

Observation of Live Cells

Living cells grown on coverslips were mounted on depression slides in 200 μl of growth medium. Preparations were sealed with Valap (1:1:1 mixture of Vaseline, lanolin, and paraffin wax) and viewed for extended time periods in an air curtain to maintain the cells at 37°C. For perfusion experiments, solutions containing anti-microtubule agents or methanol were applied to one side of a coverslip elevated on a standard microscope slide with two strips of parafilm. A channel was made in the Valap and the applied solution was drawn through the channel by capillary action using filter paper.

Anti-Microtubule Drug Treatments

Cells grown on glass coverslips were incubated in the presence of 10 μg/ml nocodazole (diluted from a 1 mg/ml solution made in DMSO) for up to 2.5 h. For taxol treatment, a 10 mM solution in DMSO was diluted to a final concentration of 10 μM and applied to cells for 4–6 h. After drug treatment, cells expressing GFP-chimeras were either observed directly, or after fixation for 7 min in 100% dry methanol at −20°C.

Chemical and Immunostaining

Cells were fixed in methanol as described above for all antibody staining. After fixation, cells were washed three times in an equal volume of PBS at pH 6.8. Incubation with primary and secondary antibodies was performed in a humid chamber at 37°C for 1 h. All antibody incubations were followed by 20-min washes in PBS + 0.01% Tween 20. mAb against α-tubulin (Amersham Corp., Arlington Heights, IL) was used at 1:500 dilution and the 12CA5 monoclonal (Babco) was used at a 1:250 dilution. All secondary antibodies (Jackson Immunoresearch Laboratories, West Grove, PA) were used at 1:100 dilutions.

Microscopy/Image Analysis

Most images were obtained using conventional Nikon (Nikon Inc., Melville, NY) or Zeiss microscopes equipped with standard fluorescein filter sets and using a Zeiss 100× planachromat lens (Carl Zeiss, Inc., Thornwood, NY). GFP images were either photographed directly on Kodak T-Max 400 film (exposures of 2 s to 1 min) or captured using a SIT camera and transferred to Image-1 software (Universal Imaging, West Chester, PA). Hard copies of stored images were obtained by formatting slides from Adobe Photoshop TIFF files and printing color photographs either from internegatives or directly using a Fuji 200II Pictrostat printer (Fuji Medical Systems, Stamford, CT). Comparative analyses of noncalibrated fluorescence intensity were carried out using Image-1 software. In brief, images of individual cells from the same coverslip were taken using a SIT camera with values for voltage, gain and black level preset at appropriate values to accommodate a range of fluorescence intensities without saturating the camera. Images of cells were taken after photoactivation of GFP had occurred. For each cell, both the total area and the total pixel density were measured and used to calculate the pixel intensity per area.

Confocal images were obtained using a Bio-Rad MRC-1000 Confocal System (Bio-Rad Labs, Richmond, CA) and a Nikon Diaphot microscope equipped with a Nikon 60× water immersion objective. Excitation was with the 488 line of a krypton-argon laser operating at 1% power. Images presented in the paper were generated from two consecutive 0.8-s scans of a single Z axis. Images were obtained at SUNY Buffalo with the invaluable assistance of Dr. R. Summers (SUNY Buffalo) and Mr. C. Blanchard (Bio-Rad Labs., Richmond, CA).

Results

Expression Constructs and General Observations

To examine the behavior of MAP 4 and its subdomains, mammalian expression vectors were constructed encoding the sequences of interest. The region of MAP 4 expressed and the type of reporter used for each construct are illustrated in Fig. 1. All sequences were inserted downstream from the cytomegalovirus promoter for high level expression in mammalian cells. Constructs were introduced into multiple cell types via liposome-mediated transfection or, less frequently, by microinjection. Results were similar for any given construct regardless of either the method of introduction of plasmid or the cell type used. Although the majority of images shown here were obtained with GFP-chimeras, similar results were seen for the same domains using HA-tagged constructs. In most cases, transcription was generically increased by addition of sodium butyrate to the tissue culture medium. However, the presence or absence of sodium butyrate had no effect on the general phenotypes observed.

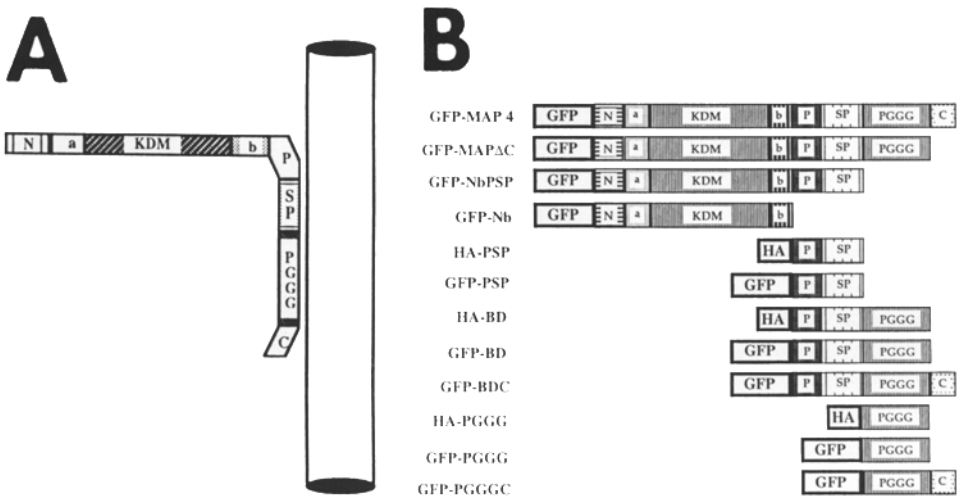

Figure 1. Schematic representation of chimeric proteins produced by eukaryotic expression vectors. (*A*) Representation of MAP 4 protein showing the basic domains attached to the surface of the microtubule, and the acidic domains projecting from the surface. (*B*) The portion of MAP 4 made and the reporter tag (*GFP* or *HA*) present at the amino terminus are shown. Designation of regions is based on the analysis presented in West et al. (63).

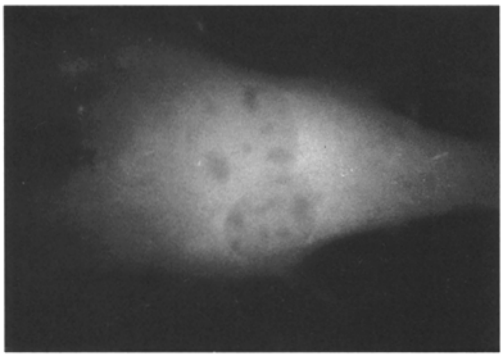

Figure 2. Live BHK cell transfected with GFP. Cells were transiently transfected with the GFP construct and then treated for 24 h with 2 mM sodium butyrate. Note the distribution of fluorescence in both cytoplasm and nucleus, although the nucleoli largely exclude the construct.

GFP-MAP 4 Is Specifically Localized to Microtubules while GFP Alone Distributes Evenly throughout the Cell

We asked whether GFP could be used as a reporter of MAP behavior in living cells by making a GFP fusion with full-length mouse MAP 4 and comparing its localization to that of a construct encoding GFP alone. The plasmids were introduced into a variety of cell types by transient transfection. Stable cell lines of CHO and BHK expressing GFP-MAP 4 were also isolated using the neomycin resistance marker on the pRc/CMV plasmid.

Cells transfected with a construct encoding GFP alone displayed diffuse fluorescence throughout the cytoplasm and nucleus (Fig. 2). These data indicate that GFP is expressed well in mammalian cells, as had been previously demonstrated both in invertebrates and bacteria (19, 61). The presence of GFP in both the nucleus and the cytoplasm also suggested that specific distributions of chimeric molecules in either of these compartments would be readily detectable. After 24 h, clonal populations of green cells could be identified, indicating that expression of GFP had no adverse effect on cell division.

Illumination of transfected cells often caused the fluorescence to intensify ~5–10 fold within a few seconds. High-level fluorescence was then maintained for several minutes before significant bleaching was seen. This observation, which pertained to GFP and all of the GFP-MAP 4 chimeras, suggests that this reporter may be useful in photoactivation assays.

Cells transfected with a fusion of GFP to full-length MAP 4 showed fluorescent arrays typical of the interphase microtubules in these cells (Fig. 3). The patterns were similar in cells that contained little (CHO; Fig. 3 *D*) or substantial (BHK; Fig. 3, *A–C*) amounts of endogenous MAP 4; they were also similar in stable or transient transfectants. In contrast to observations with GFP alone, no diffuse labeling of the cytoplasm or nucleus was observed. Arrays typically originated from a focus reminiscent of a centrosome (Fig. 3, *B* and *C*). Thus, the patterns were characteristic of normal microtubule arrays and resembled those seen previously in immunofluorescent analyses of CHO cells stably expressing human MAP 4 (3). Labeling of spindles indicated that the GFP-MAP 4 was also localized to mitotic microtubules (data not shown), as expected based on the distribution of endogenous MAP 4. The absence of microtubule abnormalities in the presence of GFP-MAP 4 expression is consistent with our previous analyses using untagged human MAP 4 expressed in CHO cells (3), and further indicates that GFP protein does not interfere with normal cellular functions detectable in these assays. In the stable transfectants, however, we noted that fluorescence intensity varied significantly between individual cells, even those of clonal origin. These results may reflect a physiologically significant property of chimera expression (variation during cell cycle, etc.), or could be due to variations in the rate at which newly synthesized GFP folds to generate a fluorescent molecule.

To confirm that the GFP-MAP 4 chimera was on microtubules, cells that were stably or transiently transfected with GFP-MAP 4 were injected with rhodaminated tubulin. As shown in Fig. 4, the signals are coincident, with microtubules labeling evenly along their length with the MAP 4 fusion protein.

The utility of GFP-chimeras for following dynamic events of the cytoskeleton in vivo is illustrated in Fig. 5. Confocal images of an optical section of a BHK cell expressing GFP-MAP 4 were taken 30 s apart; changes in individual microtubules can be readily visualized. Over the several minutes this or other cells were imaged using confocal laser scanning, there was no loss of fluorescence intensity or apparent effect on cell viability. These data are similar to those we obtained on GFP constructs using conventional fluorescence microscopy. Unlike proteins that have been covalently modified with fluorescein-based fluorophores (56), the level of GFP fluorescence does not diminish significantly during image acquisition; for our ex-

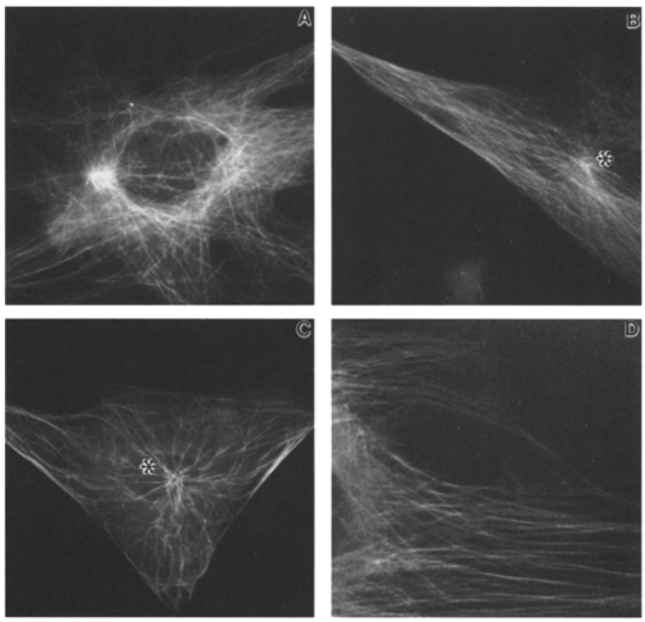

Figure 3. Images of live cells stably or transiently transfected with the GFP-MAP 4 construct. BHK (*A–C*) or CHO (*D*) cells were either transiently (*A* and *B*) or stably (*C* and *D*) transfected with GFP-mouse MAP 4. Fluorescence is localized to microtubule arrays, and no diffuse cytoplasmic signal is present. Asterisks indicate positions of microtubule organizing centers.

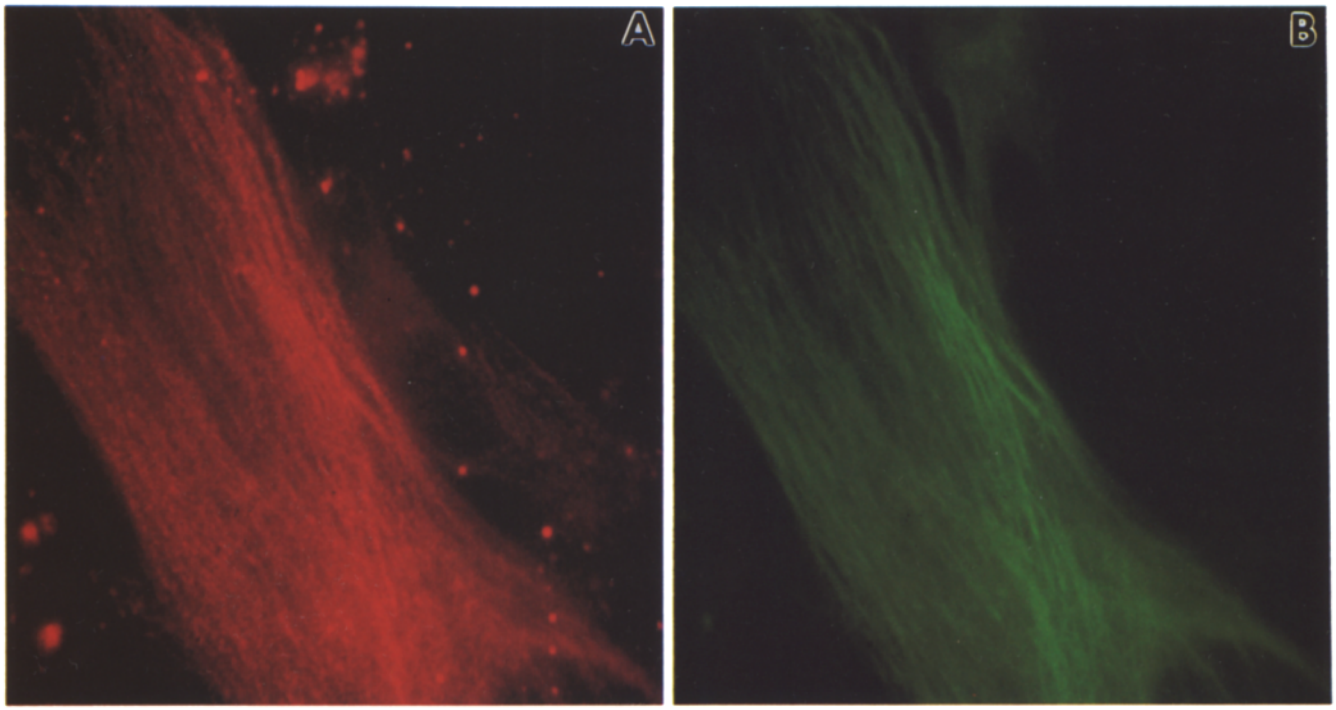

Figure 4. Colocalization of MAP 4 and tubulin in a live BHK cell. BHK cells were transiently transfected with the GFP-MAP 4 construct and incubated at 37°C for 24 h to allow expression of the vector. Cells were then microinjected with a solution containing 1 mg/ml rhodaminated tubulin and allowed to recover overnight before observation. Visualization of both rhodamine-tubulin (*A*) and GFP-MAP 4 (*B*) shows that the patterns are coincident.

periments with conventional microscopes, the use of low light-level imaging was optional. Further, cells that had been continuously illuminated for photography for periods as long as 1 min were observed to undergo cell division during the next 24-h period, suggesting negligible phototoxicity under the conditions of these observations.

These initial experiments demonstrated the utility of the GFP constructs for studying the subcellular dynamics of MAP 4 and associated structures in vivo, and led to further investigations of MAP 4 subdomains using this technology. Our analyses are detailed further in the following sections, but two points are of particular note. First, the cellular distribution of GFP chimeras was similar to what we observed previously using epitope-tagging methods; an example of one of the HA-tagged constructs is shown subsequently (see Fig. 7). However, because the cells were not processed for immunostaining, it was possible to assess the distribution of protein in localized and nonlocalized states without the uncertainties that accompany fixation. Second, correlations could be made between degrees of MAP-induced perturbation and the expression level for each construct, since the intensity of fluorescence served as an indicator of the concentration of the chimera.

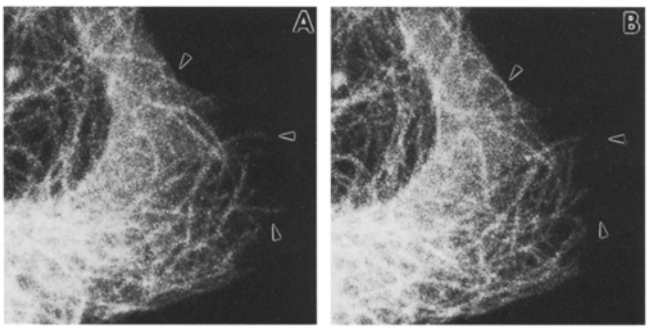

Figure 5. Dynamics of GFP-MAP 4 expressed in a stably transfected BHK cell. Images were recorded using confocal microscopy as outlined in Materials and Methods. *B* shows the same optical section as in *A*, but was recorded 30 s later. Arrows point to some of the regions in which changes in GFP-MAP 4 organization are evident.

The MAP 4 Basic Domain Causes Microtubule Rearrangements

We initiated examination of MAP 4 domains by generating GFP chimeras containing the entire basic domain. Fig. 6 illustrates that this construct (GFP-BD) causes unique, cell-type independent rearrangements of the microtubule cytoskeleton. There is a range of phenotypic abnormalities, including microtubule bundles (Fig. 6, *C* and *D*), whorls of microtubules around the nucleus (Fig. 6 *C*) and more rarely, polygonal arrays with noncentrosomal foci (Fig. 6 *B*). A few cells in each preparation appeared more or less normal (Fig. 6 *A*). The diverse effects elicited by GFP-BD expression suggested that the extent of microtubule reorganization might reflect differences in expression levels of the chimera. To test this interpretation, we correlated the amount of GFP-fluorescence with the extent of microtubule rearrangement. Using a semiquantitative measure of relative fluorescence, we determined that cells displaying the most severe bundling of microtubules had fluorescence intensities 2.5–3-fold higher than less per-

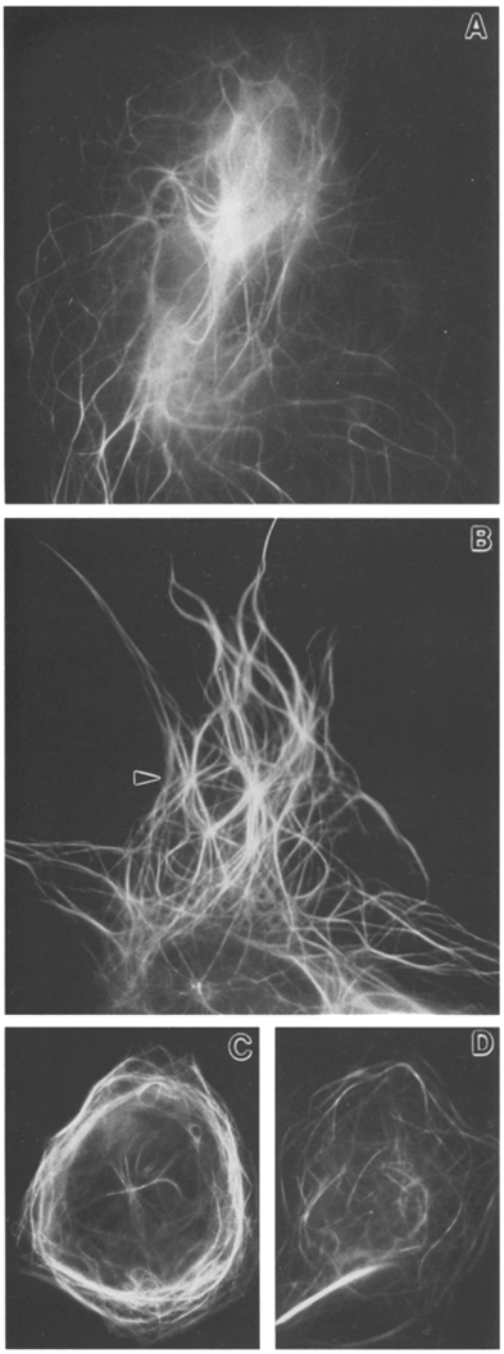

Figure 6. Living cells transiently and stably transfected with GFP-BD construct. (*A*) Stably transfected BHK cell expressing a low level of chimeric protein; no butyrate treatment. (*B*) Transiently transfected BHK cell expressing high levels of chimeric protein; treated for 2 mM sodium butyrate for 36 h. The arrow points to an area rearranged into a lattice from an apparently noncentrosomal region. (*C*) Transiently transfected Cos-7 cell, treated as in *B*. (*D*) Transiently transfected BHK cell expressing high levels of chimeric protein; treated with 2 mM sodium butyrate for 24 h. Note the extensive rearrangement of microtubules in the cells expressing higher amounts of chimeric protein.

turbed cells. Cells with very low overall fluorescence, such as shown in Fig. 6 *A*, contained more normal microtubule arrays. These data suggest that the severity of the phenotype is related to the level of transgene expression, although the factors regulating the formation of bundles versus polygonal arrays are not known. As with the full-length MAP 4, however, diffuse fluorescence was never seen with the GFP-BD construct, indicating that both these chimeric proteins have a high affinity for microtubules.

The rearrangements seen with GFP-BD were identical to those observed by immunofluorescence in a variety of cell types transfected with the basic domain tagged at its amino terminus with the nine–amino acid HA epitope (Fig. 7). These data suggest that the rearrangements are specific to the basic domain of MAP 4 and are independent of the reporter used to detect them. Comparisons made for a number of constructs (see Table I for summary) yielded similar conclusions on the innocuous nature of the larger GFP reporter versus the small epitope tag on the in vivo behaviors of the chimeras.

Separation of the Basic Domain into PSP and PGGG Components Indicates Distinct Microtubule Binding Contributions for Each Region

To examine the individual regions within the basic domain, we generated constructs containing either the MAP 4 unique flanking sequence (GFP-PSP) or the PGGG repeat domain conserved with MAP 2 and tau (GFP-PGGG). The GFP-PSP chimeric protein caused microtubule rearrangements reminiscent of those observed with the entire basic domain, but displayed a lower affinity for microtubules, as indicated by the distribution of fluorescence in both localized and diffuse states (Fig. 8 *A*). The majority of fluorescence was localized to the most severely rearranged microtubules. These results are similar to our observations using the same MAP fragment tagged with the HA epitope, although diffuse fluorescence was not observed in this latter case because of extraction of the unbound molecules during processing for immunostaining (data not shown; see also Table I). As with the intact binding domain, the PSP region displayed increased phenotypic severity at higher expression levels. Since the overall fluorescence levels of cells expressing GFP-PSP were equivalent to those containing GFP-BD constructs, we conclude that the less severe phenotype observed reflected a decreased affinity of GFP-PSP for microtubules.

Cells transfected with GFP-PGGG showed a largely nonlocalized fluorescence, regardless of expression level (Fig. 8 *B*). Decoration of microtubules was extremely rare, and the cells resembled those transfected with GFP alone. These observations are consistent with in vivo results for the PGGG repeats of MAP 2 and tau (37, 44), but they contrast with in vitro results that show an affinity of these domains for microtubules (6, 15, 22, 27, 29). Our observations with the GFP-PSP and GFP-PGGG chimeras in vivo suggest that the high affinity microtubule binding seen with the entire basic domain results from enhanced binding generated by a combination of the PSP and PGGG regions.

The Acidic Carboxy Terminus of MAP 4 Affects the Interaction of the Protein with Microtubules

Because the acidic COOH-terminal domain of MAP 4 is

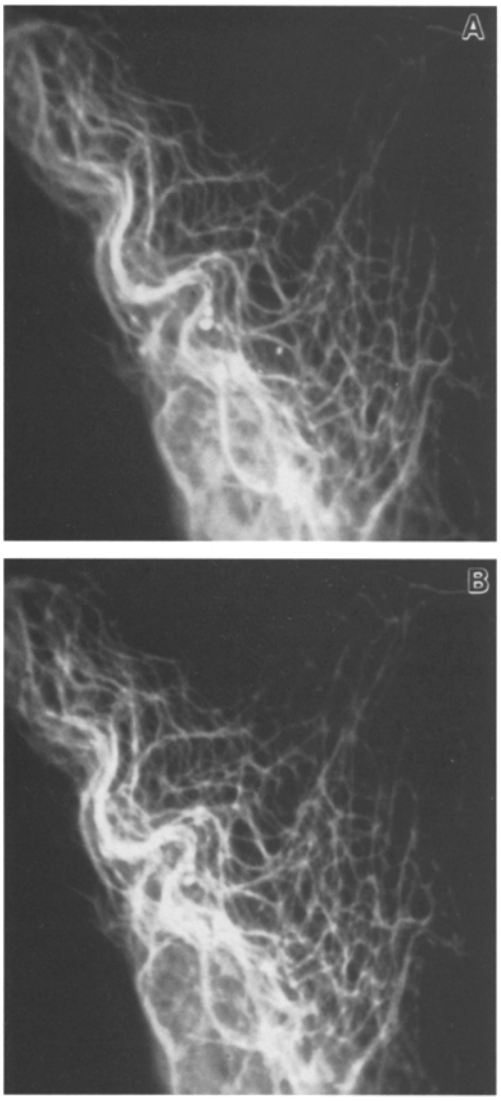

Figure 7. Double-immunofluorescence staining of BHK cells transfected with epitope tagged MAP 4 binding domain. Cells transiently transfected with HA-tagged basic domain were double-stained for tubulin with a mAb to α-tubulin and the epitope tag with the 12CA5 mAb. Tubulin staining was visualized with a secondary antibody conjugated to Texas Red (*A*), and the MAP 4 binding domain with a secondary antibody conjugated to fluorescein (*B*). The binding domain of MAP 4 is coincident with microtubules.

highly conserved among species, we examined the effect of its removal or addition on microtubule binding and organization. Surprisingly, the patterns obtained upon transfection of GFP-MAPΔC (Fig. 9 *A*) were distinct from those obtained previously with full-length MAP 4 (compare to Fig. 3). Whereas the intact protein showed normal microtubule binding and organization at all levels of expression, removal of the COOH-terminal region resulted in a moderate bundling phenotype. The frequency of microtubule bundling was high, but the phenotype was not as severe or as extensive as that seen with the GFP-BD construct. Polygonal arrays of noncentrosomal microtubules were occasionally seen, and diffuse signal was never observed. These results demonstrate that removal of the acidic COOH-terminal domain, comprising less than 6% of the entire MAP 4 protein, still allows tight binding to microtubules, but modulates the activity of the MAP with respect to microtubule organization.

Table I. Summary of Transfection Results with GFP Expression Vectors

Construct	MT binding	MT bundling	Diffuse labeling
GFP	−	−	++++
GFP-MAP4	++++	−	−
GFP-MAPΔC	++++	++	−
GFP-NbPSP	++++	−	−
GFP-Nb	−	−	++++
GFP-PSP	+++	+++	++
GFP-BD	++++	++++	−
GFP-BDC	++++	+++	−
GFP-PGGG	±	−	+++
GFP-PGGGC	−	−	++++
HA-BD	++++	++++	−
HA-PSP	++	++	−
HA-PGGG	±	−	−
HA-PGGGC	−	−	−

Pluses and minuses are arbitrary designations to indicate the relative activity of the GFP chimeras. See text for a discussion of the differences between the GFP and HA-tagged PSP construct.

An effect of the COOH-terminal domain on MAP 4 binding is confirmed and extended in experiments that combine this region with portions of the basic domain. Transfectants expressing the GFP-BDC construct showed microtubule rearrangements more similar to the BD phenotype than MAPΔC (Fig. 9 *B*), although bundles were generally smaller and thinner and rearrangements were less dramatic. As with the MAPΔC protein, GFP-BDC showed no diffuse labeling, indicating that the microtubule affinity of the chimeras had not been significantly diminished. However, the subtle differences in microtubule rearrangements observed for GFP-BDC without any alteration in expression level again suggest a regulatory role for the COOH-terminal domain. This notion is further supported in transfections with the GFP-PGGGC construct, shown in Fig. 9 *C*, where labeling was entirely diffuse, and the rare labeling of microtubules seen with the GFP-PGGG construct was never observed. Collectively, comparisons of microtubule rearrangements seen in chimeric proteins with or without the acidic COOH-terminal domain suggest that this domain modulates interactions of the basic domain with microtubules, possibly as a result of its negative charge.

The Projection Domain Shows No In Vivo Association with Microtubules, but Is Able to Regulate Interaction of the Basic Domain with Microtubules

To identify the role of the projection domain in MAP 4 function and/or microtubule binding, we used the GFP-Nb construct encoding the entire acidic projection domain extending from the amino terminus of MAP 4 to the border of the basic region. Cells transiently transfected with GFP-Nb displayed diffuse labeling, and showed no interaction with microtubules, regardless of expression level (Fig. 10 *A*). Unlike the nonlocalized distribution seen with GFP alone, however, the projection domain chimera is ex-

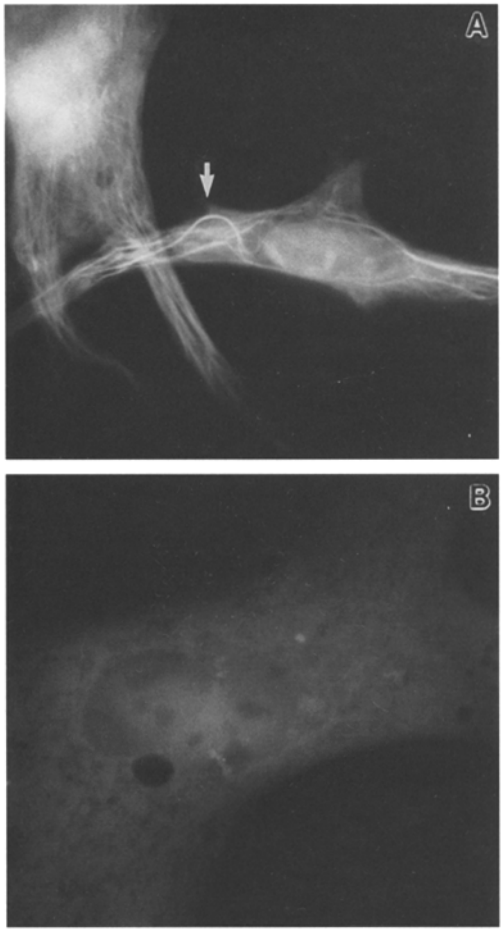

Figure 8. Live BHK cells transiently transfected with GFP-PSP or GFP-PGGG constructs. (*A*) Cell transfected with the GFP-PSP construct. The arrow in *A* points to a prominent microtubule bundle within the cell. (*B*) Cell transfected with the GFP-PGGG construct; note the diffuse labeling. Cells shown were treated with sodium butyrate for 36 h.

cluded from the nucleus, presumably because of its large size. The failure of GFP-Nb to associate with microtubules implies that the projection domain does not form dimers with endogenous MAP 4. Whether other MAPs dimerize has been debated (see references 14 and 64).

We next sought to determine the effect of the projection domain on interaction of the PSP region with microtubules. Transfections with the GFP-NbPSP construct revealed that the chimeric protein associates with microtubules in a manner indistinguishable from that of full-length MAP 4, despite missing both the PGGG repeats and COOH-terminal domain (Fig. 10 *B*). This was a surprising result, as a chimera containing the projection domain and basic binding domain (GFP-MAPΔC) showed distinct microtubule reorganization. Interestingly, the diffuse labeling observed previously with the GFP-PSP chimera was absent with the GFP-NbPSP construct. These data suggest that the projection domain is capable of increasing the affinity of the PSP region for microtubules, but without causing the reorganization of microtubules into bundles.

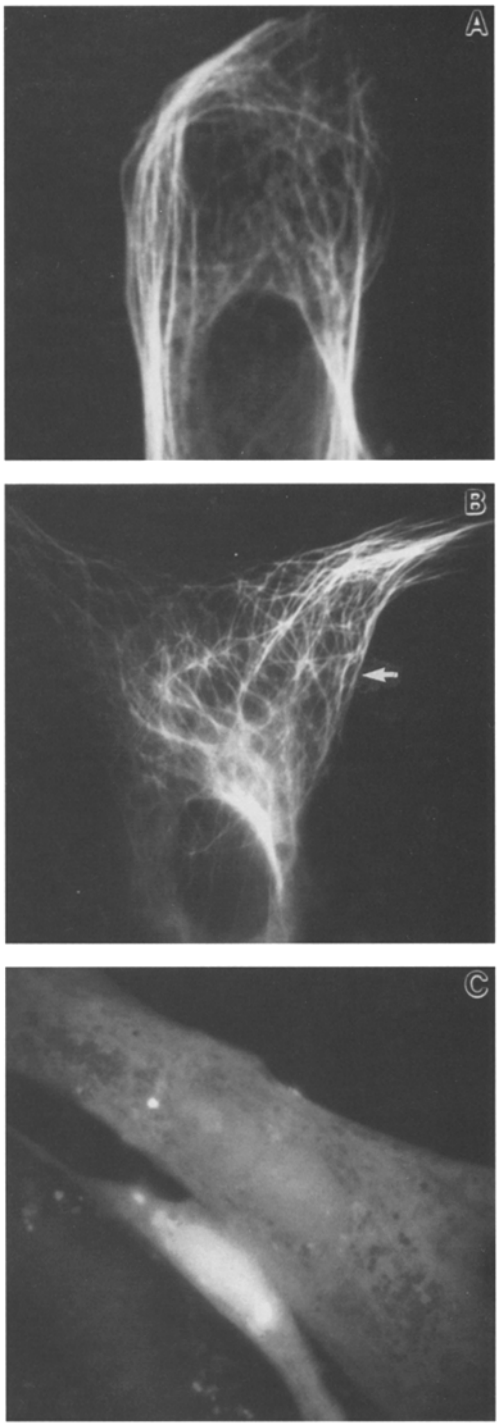

Figure 9. Live BHK cells transiently transfected with GFP-MAPΔC, GFP-BDC or GFP-PGGGC constructs. (*A*) GFP-MAPΔC; (*B*) GFP-BDC; (*C*) GFP-PGGGC. The arrow in *B* indicates microtubules arranged in a polygonal lattice. All cells shown were treated with sodium butyrate for 24 h.

Treatment of Transfectants with Nocodazole Demonstrates Enhanced Stability of Microtubule Bundles in the Presence of the GFP-BD and GFP-PSP

We have observed distinct microtubule binding activities for the different MAP 4 constructs studied here, some of which were characterized by the appearance of microtu-

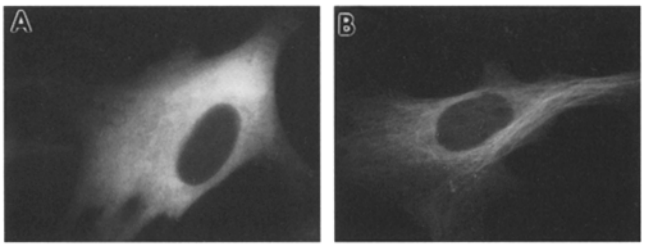

Figure 10. Live BHK cells transiently transfected with GFP-Nb or GFP-NbPSP vectors encoding the acidic projection domain. (*A*) GFP-Nb; (*B*) GFP-NbPSP. Cells were treated with sodium butyrate for 24 h. Note the absence of localization of fluorescence in *A*, and the strong localization to microtubules in *B*.

bule bundles. A plausible hypothesis is that the microtubule bundling seen with some of the constructs is a result of preferential stabilization of microtubules. To test this idea, we asked if different classes of microtubules could be distinguished by their sensitivity to microtubule depolymerizing drugs. BHK cells stably expressing either GFP-MAP 4 or GFP-BD were incubated with 10 μg/ml nocodazole for up to 60 min, and live cells were observed for the presence of stable microtubules. Cells expressing GFP-MAP 4 or GFP-BD were observed every minute for several minutes to follow the nocodazole-mediated depolymerization of microtubules. As shown in comparing Fig. 11, *A* and *C*, all the cellular microtubules in a cell expressing GFP-MAP 4 were depolymerized within 5 min of treatment. This is consistent with previously published results indicating that MAP 4 does not have a stabilizing effect in cells treated with anti-mitotic agents (3). In contrast, cells expressing GFP-BD displayed two readily distinguishable populations of microtubules. As shown in comparing Fig. 11, *B* with *D*, microtubules that were not bundled depolymerized within 5 min, whereas those in bundles persisted. The bundle shown was still present after 30 min of observation, and bundles were observed in other cells after as long as 1–2 h of drug treatment. These data are consistent with experiments in which HA-tagged BD and microtubule patterns were compared by double immunofluorescence; these also showed that only bundled microtubules persisted after treatment with nocodazole. Real-time experiments demonstrated that the bundles produced by the GFP-PSP fusion protein were also stabilized against depolymerization (data not shown). Thus, bundling caused by certain MAP 4 protein domains is correlated with microtubule stabilization.

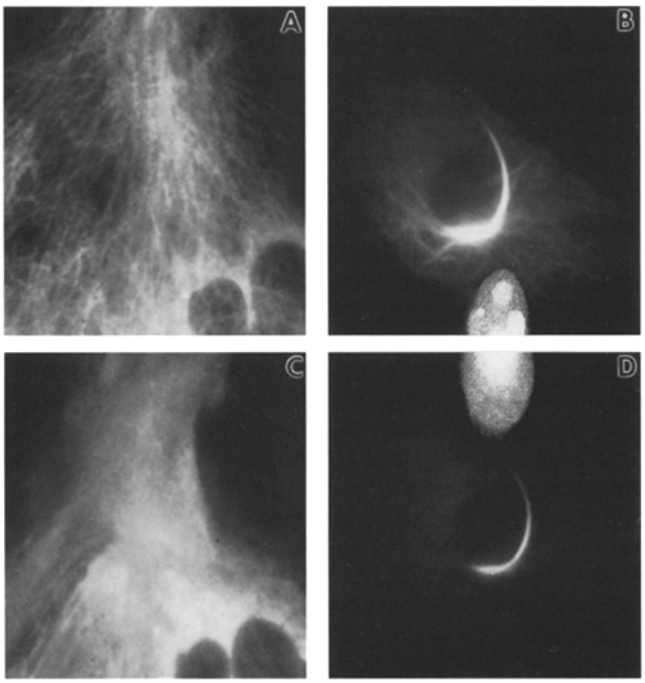

Figure 11. Differential resistance of microtubules to nocodazole in cells transfected with MAP 4 or the basic domain. BHK cells transfected with either GFP-MAP 4 (*A* and *C*) or GFP-BD (*B* and *D*) were imaged before treatment (*A* and *B*) or after treatment with 10 μg/ml nocodazole for 5 min (*C* and *D*). Note the depolymerization of single microtubules in both *C* and *D*, but the persistence of the microtubule bundle in *D*.

Treatment of transfectants with taxol (10 μM taxol for 4–6 h) showed that the GFP chimeras generally followed the aberrant microtubule patterns generated by this drug (data not shown). Interestingly, GFP-PGGG protein showed a higher degree of association with the taxol-stabilized microtubule bundles than in nontreated cells. These data suggest that the GFP-PGGG chimera is functional in microtubule binding, but has a lower affinity for dynamic microtubules.

Discussion

Results presented here demonstrate that GFP is an effective reporter for subcellular structures like the cytoskeleton, providing good temporal and spatial resolution in living cells. We have used this reporter to show that GFP-MAP 4 mimics the behavior of both intact MAP 4 (3) and portions of MAP 4 tagged with an HA epitope, providing encouraging evidence that GFP, despite its 27-kD size, is a benign tag for studying the behavior of at least some proteins in vivo. The efficacy of GFP for such analyses is due partly to its relatively stable, high-intensity fluorescence that can be imaged in living cells using standard microscopic equipment. GFP phototoxicity and photobleaching are low, so cell physiology appears unimpaired during observation. Moreover, the fluorescence of GFP, visualized with fluorescein filters, increases over the first 30 s of examination, facilitating its use as a tag and suggesting the possibility of photoactivation experiments (e.g., reference 52) for the study of binding kinetics. The ability to visualize both MAP 4 and microtubules, through the use of rhodaminated tubulin injected into cells containing GFP-MAP 4 constructs, also opens the possibility of performing experiments in which the dynamics of these elements can be analyzed simultaneously. This work extends the pioneering studies of GFP as a tag for protein behavior (19, 61) and echoes newly reported work on ion channel chimeras that shows the utility of GFP as an indicator of expression levels (48).

Our utilization of GFP for the dissection of MAP 4 domain behavior has revealed that interaction of this protein with microtubules is complex, and is modulated by sequences both within and outside the basic domain required for microtubule binding (see Table I). Further, these studies have provided new evidence for the distinc-

tive behavior of MAP 4 in vivo compared with other structural MAPs. Full-length GFP-MAP 4 chimeras, either transiently or stably introduced into cells, localized to microtubules and caused no microtubule reorganization in interphase or mitotic cells. In agreement with our previous findings (3), GFP-MAP 4 expression had no effect on the sensitivity of microtubules to depolymerizing drugs. One function often attributed to the structural MAPs, including MAP 4 (8) is stabilization of microtubule arrays (3, 6, 32, 37, 42, 45, 50, 62). Our data indicate that despite some overall structural similarities and strong sequence conservation of the PGGG repeats among MAP 2, tau and MAP 4, MAP 4 in cycling cells is distinct from the neural MAPs in its effects on microtubule organization and dynamic instability.

Our results show that the entire basic domain of MAP 4 causes extensive rearrangement of microtubule arrays into bundles, stabilization of these bundles against depolymerization and, in rare instances, formation of polygonal lattices. The formation of bundles is similar to findings from the heterologous expression of analogous regions of MAP 2 (39) and tau (6, 37), whereas the formation of the polygons is unique to MAP 4. Bundling in itself is a complex phenomenon (see reference 14) and there is some debate over whether the bundling observed with the neural MAPs may be a result of microtubule cross-bridging. Recent in vitro studies (29) indicate that tau-induced bundling occurs in the absence of cross-linking, implicating other factors such as promotion of microtubule assembly and stabilization or neutralization of negative charge on the tubulin polymer. Our data are most consistent with a bundling model based on increased stability and assembly of microtubules in the presence of GFP-BD and GFP-PSP.

These in vivo studies showed that within the basic domain, the PSP domain, unique to MAP 4, binds strongly to microtubules and induces their bundling, whereas the highly conserved PGGG repeat region has a low affinity for dynamic microtubules and is dispensable for normal microtubule binding. In vitro experiments with MAP 4 have indicated that a region upstream from the PGGG repeats has a higher affinity for microtubules than the repeats themselves, and can generate aberrant tubulin polymers unless linked to the PGGG repeats (1). The low affinity of either intact or individual PGGG repeats for microtubules has previously been observed for tau and MAP 2 both in vitro and in vivo (15, 24, 27, 29, 35). Our experiments indicate that the binding of the PGGG repeats is enhanced when microtubules are stabilized by taxol-treatment and thus that dynamic microtubules are poor substrates for its binding. In concert with the PSP domain, however, a strong binding interaction occurs. These data are consistent with a current model for tau binding to microtubules in vitro that suggests that regions flanking the PGGG repeats act as "jaws" that aid in the placement and binding of the repeats (29). Investigations are currently underway to determine whether the conserved phosphorylation sites that lie within the PSP domain, and that include a cdc2 site, may modulate these binding interactions in vivo.

Our analysis of the MAP 4 projection domain (GFP-Nb) indicated that it does not itself associate with microtubules, but strongly modulates the activity of the binding domain. Although MAP 4 can dimerize in solution (11), the diffuse cytoplasmic distribution of this domain suggests that this interaction does not occur in vivo. The absence of binding is also consistent with in vitro studies in which a proteolytic fragment (1) or a bacterially expressed protein (West and Olmsted, unpublished data) corresponding to this acidic domain showed no affinity for microtubules. The projection domain had an unexpected influence, however, on the interaction of the PSP domain with microtubules. Cells transfected with GFP-NbPSP displayed high-affinity microtubule binding identical to that seen with intact MAP 4, with no polymer rearrangements or diffuse labeling. This contrasts with the PSP domain alone, which was capable of generating and binding to microtubule bundles as well as existing in a nonlocalized state. Our results with this domain differ from those obtained with an analogous region of tau, which was unable to bind microtubules in vivo (44), and bound with only very low affinity (K_d of $\geq$s1 mM) in vitro (29). Collectively, these data indicate that the nonconserved acidic regions of different structural MAPs account for their unique behaviors.

One way in which the projection domain might exert its influence on the binding domain other than through direct interaction with the microtubule surface is via post-translational modifications. Others have shown that phosphorylation of MAP 2 decreases its affinity for microtubules (7) and that the protein structure of tau stiffens upon phosphorylation, a process that could influence the affinity of the molecule for microtubules (4, 30, 47). The projection domain of MAP 4 has multiple (>50) potential sites for phosphorylation by cAMP-dependent kinase and casein kinase II. Although it has been shown that cell cycle-dependent phosphorylation of MAP 4 occurs, presumably by cdc2 kinase (59, 60), whether these other sites are significant in the modulation of MAP 4 activity remains to be determined.

While addition or removal of the large projection domain might have been predicted to affect the behavior of MAP 4, it was surprising that the small acidic COOH-terminal domain had a pronounced influence on MAP-microtubule interaction. This carboxy terminus is highly conserved (90%) (63) in MAP 4 across species. A similar region is found in MAP 2 and tau, and while conserved for any given structural MAP, collectively these domains do not strongly resemble one another. In vivo and in vitro analyses with tau have shown that the carboxy terminus enhances both association of the binding domain with microtubules and bundling (6, 37). Our results with MAP 4 constructs are in direct contrast to those seen with tau. In cases where the carboxy terminus was included within a construct (e.g., GFP-BDC or GFP-PGGGC), there was a general decrease in either microtubule reorganization or microtubule binding, respectively, with no corresponding increase in the amount of nonlocalized signal. Conversely, deletion of the carboxy terminus from full-length MAP 4 (less than 6% of the protein) resulted in mild reorganization of microtubules and variable amounts of microtubule bundling. These results all suggest that the acidic COOH terminus plays a significant role in the interaction of the binding domain with microtubules, but whether this is due to charge or steric interactions is not yet resolved.

Our transfection results for the various domain constructs of MAP 4 (summarized in Table I) lead to a model for the association of this protein with microtubules in vivo. The entire basic region of MAP 4 is directly involved in microtubule binding, with the nonconserved PSP flanking sequence serving as the primary association domain. This domain alone is able to bind to microtubules and stabilize them against depolymerization with nocodazole, although with lower activity than the intact binding domain. In the presence of the projection domain, the PSP region is able to perform as a functional microtubule binding domain with characteristics indistinguishable from the full-length protein in the assays used here. We propose that the PSP domain directs MAP 4 to the surface of microtubules, and that the PGGG repeats may then enhance binding, but are themselves unable to bind efficiently in vivo. This implies that the PGGG repeats serve some other function associated with microtubule assembly, such as stabilization of assembled tubulin dimers. Once bound to the microtubule surface, the basic domain can alter existing arrays of microtubules in a dominant negative fashion if not properly regulated. Addition of either acidic domain of MAP 4 (the projection domain or the COOH terminus) to the basic region modifies this interaction. Studies are currently in progress to determine how some of the tissue-specific splicing variants and posttranslational modifications that occur in various regions of MAP 4 may contribute to the overall regulation of the molecule. With the development of GFP-MAP 4 chimeras and stable cell lines, and with the ability to visualize MAP on rhodaminated microtubules, it will also now be possible to test directly how these modifications influence the dynamics of both MAPs and microtubules in vivo.

We thank Dr. M. Chalfie for the gift of the GFP plasmid; Drs. L. Angerer, R. Angerer, M. Gorovsky, E. Vaisberg and R. West for critical reading of the manuscript; and H. D. Lyon for technical assistance. Dr. R. Summers (SUNY Buffalo) and Mr. C. Blanchard (Bio-Rad Labs.) provided invaluable help in obtaining the confocal images.

This work was supported by National Institutes of Health GM22214 and National Science Foundation GER 9350145 to J. B. Olmsted and National Institutes of Health GM36663 to J. R. McIntosh.

Received for publication 8 March 1995 and in revised form 18 April 1995.

References

1. Aizawa, H., Y. Emori, A. Mori, H. Murofushi, H. Sakai, and K. Suzuki. 1991. Functional analyses of the domain structure of microtubule-associated protein-4 (MAP-U). *J. Biol. Chem.* 266:9841–9846.
2. Andersen, S. S. L., B. Buendia, J. E. Dominguez, A. Sawyer, and E. Karsenti. 1994. Effect on microtubule dynamics of XMAP230, a microtubule-associated protein present in *Xenopus laevis* eggs and dividing cells. *J. Cell Biol.* 127:1289–1299.
3. Barlow, S., M. L. Gonzalez-Garay, R. R. West, J. B. Olmsted, and F. Cabral. 1994. Stable expression of heterologous microtubule-associated proteins (MAPs) in Chinese hamster ovary cells: evidence for differing roles of MAPs in microtubule organization. *J. Cell Biol.* 126:1017–1030.
4. Biernat, J., N. Gustke, G. Drewes, E.-M. Mandelkow, and E. Mandelkow. 1993. Phosphorylation of Ser^{262} strongly reduces binding of tau to microtubules: distinction between PHF-like immunoreactivity and microtubule binding. *Neuron.* 11:153–163.
5. Bloom, G. S. 1992. Motor proteins for cytoplasmic microtubules. *Curr. Opin. Cell Biol.* 4:66–73.
6. Brandt, R., and G. Lee. 1993. Functional organization of microtubule-associated protein tau. Identification of regions which affect microtubule growth, nucleation, and bundle formation *in vitro*. *J. Biol. Chem.* 268: 3414–3419.
7. Brugg, B., and A. Matus. 1991. Phosphorylation determines the binding of microtubule-associated protein 2 (MAP2) to microtubules in living cells. *J. Cell Biol.* 114:735–743.
8. Bulinski, J. C. 1994. MAP 4. *In* Microtubules. K. Roberts and J. S. Hyams, editors. Wiley-Liss, Inc., New York. 167–182.
9. Bulinski, J. C., and G. G. Borisy. 1980. Immunofluorescence localization of HeLa cell microtubule-associated proteins on microtubules in vitro and in vivo. *J. Cell Biol.* 87:792–801.
10. Bulinski, J. C., and G. G. Borisy. 1980. Widespread distribution of a 210,000 mol wt microtubule-associated protein in cells and tissues of primates. *J. Cell Biol.* 87:802–808.
11. Bulinski, J. C., and G. G. Borisy. 1980. Microtubule-associated proteins from cultured HeLa cells. Analysis of molecular properties and effects on microtubule polymerization. *J. Biol. Chem.* 255:11570–11576.
12. Bulinski, J. C., and A. Bossler. 1994. Purification and characterization of ensconsin, a novel microtubule stabilizing protein. *J. Cell Sci.* 107:2839–2849.
13. Bulinski, J. C., and G. G. Gundersen. 1991. Stabilization and post-translational modification of microtubules during cellular morphogenesis. *Bioessays.* 13:285–293.
14. Burgin, K. E., B. Ludin, J. Ferralli, and A. Matus. 1994. Bundling of microtubules in transfected cells does not involve an autonomous dimerization site on the MAP2 molecule. *Mol. Biol. Cell.* 5:511–517.
15. Butner, K. A., and M. W. Kirschner. 1991. Tau protein binds to microtubules through a flexible array of distributed weak sites. *J. Cell Biol.* 115: 717–730.
16. Caceres, A., and K. S. Kosik. 1990. Inhibition of neurite polarity by tau antisense oligonucleotides in primary cerebellar neurons. *Nature (Lond.).* 343:461–463.
17. Caceres, A., J. Mautino, and K. S. Kosik. 1992. Suppression of MAP2 in cultured cerebellar macroneurons inhibits minor neurite formation. *Neuron.* 9:607–618.
18. Cassimeris, L., N. K. Pryer, and E. D. Salmon. 1988. Real-time observations of microtubule instability in living cells. *J. Cell Biol.* 107:2223–2231.
19. Chalfie, M., Y. Tu, G. Euskirchen, W. W. Ward, and D. C. Prasher. 1994. Green fluorescent protein as a marker for gene expression. *Science (Wash. DC).* 263:802–805.
20. Chapin, S. J., and J. C. Bulinski. 1992. Microtubule stabilization by assembly-promoting microtubule-associated proteins: a repeat performance. *Cell Motil. Cytoskeleton.* 23:236–243.
21. Code, R. J., and J. B. Olmsted. 1992. Mouse microtubule-associated protein 4 (MAP4) transcript diversity generated by alternative polyadenylation. *Gene (Amst.).* 122:367–370.
22. Coffey, R. L., and D. L. Purich. 1995. Non-cooperative binding of the MAP-2 microtubule-binding region to microtubules. *J. Biol. Chem.* 270: 1035–1040.
23. Eddé, B., J. Rossier, J.-P. Le Caer, E. Desbruyères, F. Gros, and P. Denoulet. 1990. Posttranslational glutamylation of α-tubulin. *Science (Wash. DC).* 247:83–85.
24. Ennulat, D. J., R. K. H. Liem, G. A. Hashim, and M. L. Shelanski. 1989. Two separate 18-amino acid domains of tau promote the polymerization of tubulin. *J. Biol. Chem.* 264:5327–5330.
25. Gard, D. L., and M. W. Kirschner. 1987. A microtubule-associated protein from *Xenopus* eggs that specifically promotes assembly at the plus-end. *J. Cell Biol.* 105:2203–2215.
26. Gelfand, V. I., and A. D. Bershadsky. 1991. Microtubule dynamics: Mechanism, regulation, and function. *Annu. Rev. Cell Biol.* 7:93–116.
27. Goode, B. L., and S. C. Feinstein. 1994. Identification of a novel microtubule binding and assembly domain in the developmentally regulated inter-repeat region of tau. *J. Cell Biol.* 124:769–782.
28. Gorbsky, G. J., P. J. Sammak, and G. G. Borisy. 1988. Microtubule dynamics and chromosome motion visualized in living anaphase cells. *J. Cell Biol.* 106:1185–1192.
29. Gustke, N., B. Trinczek, J. Biernat, E.-M. Mandelkow, and E. Mandelkow. 1994. Domains of t protein and interactions with microtubules. *Biochemistry.* 33:9511–9522.
30. Hagestedt, T., B. Lichtenberg, H. Wille, E.-M. Mandelkow, and E. Mandelkow. 1989. Tau protein becomes long and stiff upon phosphorylation: Correlation between paracrystalline structure and degree of phosphorylation. *J. Cell Biol.* 109:1643–1651.
31. Harada, A., K. Oguchi, S. Okabe, J. Kuno, S. Terada, T. Ohshima, R. Sato-Yoshitake, Y. Takei, T. Noda, and N. Hirokawa. 1994. Altered microtubule organization in small-calibre axons of mice lacking *tau* protein. *Nature (Lond.).* 369:488–491.
32. Hirokawa, N. 1994. Microtubule organization and dynamics dependent on microtubule-associated proteins. *Curr. Opin. Cell Biol.* 6:74–81.
33. Holzbaur, E. L. F., and R. B. Vallee. 1994. Dyneins: molecular structure and cellular function. *Ann. Rev. Cell Biol.* 10:339–372.
34. Inouye, S., and F. I. Tsuji. 1994. Aequorea green fluorescent protein. Expression of the gene and fluorescence characteristics of the recombinant protein. *FEBS (Fed. Eur. Biochem. Soc.) Lett.* 341:277–280.
35. Joly, J. C., G. Flynn, and D. L. Purich. 1989. The microtubule-binding fragment of microtubule-associated protein-2: location of the protease-accessible site and identification of an assembly-promoting peptide. *J. Cell Biol.* 109:2289–2294.
36. Joly, J. C., and D. L. Purich. 1990. Peptides corresponding to the second repeated sequence in MAP-2 inhibit binding of microtubule-associated proteins to microtubules. *Biochemistry.* 29:8916–8920.

37. Kanai, Y., J. Chen, and N. Hirokawa. 1992. Microtubule bundling by tau proteins *in vivo*: Analysis of functional domains. *EMBO(Eur. Mol. Biol. Organ.) J.* 11:3953–3961.
38. Kanai, Y., R. Takemura, T. Oshima, H. Mori, Y. Ihara, M. Yanagisawa, T. Masaki, and N. Hirokawa. 1989. Expression of multiple tau isoforms and microtubule bundle formation in fibroblasts transfected with a single tau cDNA. *J. Cell Biol.* 109:1173–1184.
39. Kindler, S., B. Schulz, M. Goedert, and C. C. Garner. 1990. Molecular structure of microtubule-associated protein 2b and 2c from rat brain. *J. Biol. Chem.* 265:19679–19684.
40. Knops, J., K. S. Kosik, G. Lee, J. D. Pardee, L. Cohen-Gould, and L. McConlogue. 1991. Overexpression of tau in a nonneuronal cell induces long cellular processes. *J. Cell Biol.* 114:725–733.
41. Kolodziej, P. A., and R. A. Young. 1991. Epitope tagging and protein surveillance. *Methods Enzymol.* 194:508–519.
42. LeClerc, N., K. S. Kosik, N. Cowan, T. P. Pienkowski, and P. W. Baas. 1993. Process formation in Sf9 cells induced by the expression of a microtubule-associated protein 2C-like construct. *Proc. Natl. Acad. Sci. USA.* 90:6223–6227.
43. Lee, G. 1993. Non-motor microtubule-associated proteins. *Curr. Opin. Cell Biol.* 5:88–94.
44. Lee, G., and S. L. Rook. 1992. Expression of tau protein in non-neuronal cells: microtubule binding and stabilization. *J. Cell Sci.* 102:227–237.
45. Lewis, S. A., I. E. Ivanov, G.-H. Lee, and N. J. Cowan. 1989. Organization of microtubules in dendrites and axons is determined by a short hydrophobic zipper in microtubule-associated proteins MAP2 and tau. *Nature (Lond.).* 342:498–505.
46. Lewis, S. A., D. Wang, and N. J. Cowan. 1988. Microtubule-associated protein MAP 2 shares a microtubule binding motif with tau protein. *Science (Wash. DC)* 242:936-939.
47. Lichtenberg, B., E. M. Mandelkow, T. Hagestedt, and E. Mandelkow. 1988. Structure and elasticity of microtubule-associated protein tau. *Nature (Lond.).* 334:359–362.
48. Marshall, J., R. Molloy, G. W. J. Moss, J. R. Howe, and T. E. Hughes. 1995. The jellyfish green fluorescent protein: a new tool for studying ion channel expression and function. *Neuron.* 14:211–215.
49. Masson, D., and T. E. Kreis. 1993. Identification and molecular characterization of E-MAP-115, a novel microtubule-associated protein predominantly expressed in epithelial cells. *J. Cell Biol.* 123:357–371.
50. Matus, A. 1994. Stiff microtubules and neuronal morphology. *Trends Neurosci.* 17:19–22.
51. Mitchison, T., and M. Kirschner. 1984. Dynamic instability of microtubule growth. *Nature (Lond.).* 312:237–242.
52. Mitchison, T. J. 1989. Polewards microtubule flux in the mitotic spindle: evidence from photoactivation of fluorescence. *J. Cell Biol.* 109:637–652.
53. Murofushi, H., S. Kotani, H. Aizawa, S.-I. Hisanaga, N. Hirokawa, and H. Sakai. 1986. Purification and characterization of a 190 kD microtubule-associated protein from bovine adrenal cortex. *J. Cell Biol.* 103:1911–1919.
54. Olmsted, J. B. 1991. Non-motor microtubule-associated proteins. *Curr. Op. Cell Biol.* 3:52–58.
55. Olmsted, J. B., and H. D. Lyon. 1981. A microtubule-associated protein specific to differentiated neuroblastoma cells. *J. Biol. Chem.* 256:3507–3511.
56. Olmsted, J. B., D. L. Stemple, W. M. Saxton, B. W. Neighbors, and J. R. McIntosh. 1989. Cell cycle-dependent changes in the dynamics of MAP 2 and MAP 4 in cultured cells. *J. Cell Biol.* 109:211-223.
57. Parysek, L. M., C. F. Asnes, and J. B. Olmsted. 1984. MAP 4: occurrence in mouse tissues. *J. Cell Biol.* 99:1309–1315.
58. Prasher, D. C., V. K. Eckenrode, W. W. Ward, F. G. Prendergast, and M. J. Cormier. 1992. Primary structure of the *Aequorea victoria* green-fluorescent protein. *Gene (Amst.).* 111:229–233.
59. Tombes, R. M., J. G. Peloquin, and G. G. Borisy. 1991. Specific association of an M-phase kinase with isolated mitotic spindles and identification of two of its substrates as MAP4 and MAP1B. *Cell Regul.* 2:861–874.
60. Vandré, D. D., V. E. Centonze, J. Peloquin, R. M. Tombes, and G. G. Borisy. 1991. Proteins of the mammalian mitotic spindle: Phosphorylation/dephosphorylation of MAP-4 during mitosis. *J. Cell Sci.* 98:577–588.
61. Wang, S., and T. Hazelrigg. 1994. Implications for bcd mRNA localization from spatial distribution of exu protein in *Drosophila* oogenesis. *Nature (Lond.).* 369:400–403.
62. Weisshaar, B., T. Doll, and A. Matus. 1992. Reorganisation of the microtubular cytoskeleton by embryonic microtubule-associated protein 2 (MAP2c). *Development (Camb.).* 116:1151–1161.
63. West, R. R., K. M. Tenbarge, and J. B. Olmsted. 1991. A model for microtubule-associated protein 4 structure. Domains defined by comparisons of human, mouse, and bovine sequences. *J. Biol. Chem.* 266:21886–21896.
64. Wille, H., E.-M. Mandelkow, J. Dingus, R. B. Vallee, L. I. Binder, and E. Mandelkow. 1992. Domain structure and antiparallel dimers of microtubule-associated protein 2 (MAP2). *J. Struct. Biol.* 108:49–61.